Journal of Proteomics 134 (2016) 193–202

Contents lists available at ScienceDirect

Journal of Proteomics

journal homepage: www.elsevier.com/locate/jprot

Homogenization of tissues via picosecond-infrared laser (PIRL) ablation: Giving a closer view on the *in-vivo* composition of protein species as compared to mechanical homogenization

M. Kwiatkowski [a], M. Wurlitzer [a], A. Krutilin [a], P. Kiani [a], R. Nimer [a], M. Omidi [a], A. Mannaa [a], T. Bussmann [b], K. Bartkowiak [c], S. Kruber [d], S. Uschold [d], P. Steffen [a], J. Lübberstedt [a], N. Küpker [a], H. Petersen [e], R. Knecht [e], N.O. Hansen [d], A. Zarrine-Afsar [f], W.D. Robertson [d], R.J.D. Miller [d], H. Schlüter [a,*]

[a] University Medical Centre Hamburg-Eppendorf, Institute for Clinical Chemistry, Department for Mass Spectrometric Proteomics, Martinistraße 52, 20246 Hamburg, Germany
[b] Beiersdorf AG, Research & Development, Unnastrasse 48, 20245, Hamburg, Germany
[c] University Medical Centre Hamburg-Eppendorf, Department of Tumor Biology, Martinistraße 52, 20246 Hamburg, Germany
[d] Max Planck Institute for the Structure and Dynamics of Matter, Atomically Resolved Dynamics Division, Luruper Chaussee 149, 22761 Hamburg, Germany
[e] University Medical Centre Hamburg-Eppendorf, Department of Otorhinolaryngology, Head and Neck Surgery and Oncology, Martinistraße 52, 20246 Hamburg, Germany
[f] Techna Institute for the Advancement of Technology for Health, University Health Network, Toronto, ON M5G-1P5, Canada & Department of Medical Biophysics, University of Toronto, 101 College Street Suite 15-701, Toronto, ON M5G 1L7, Canada

ARTICLE INFO

Article history:
Received 30 July 2015
Received in revised form 22 December 2015
Accepted 31 December 2015
Available online 8 January 2016

Keywords:
Tissue homogenization
Protein species
Proteolysis
PIRL-DIVE
Mass spectrometry

ABSTRACT

Posttranslational modifications and proteolytic processing regulate almost all physiological processes. Dysregulation can potentially result in pathologic protein species causing diseases. Thus, tissue species proteomes of diseased individuals provide diagnostic information. Since the composition of tissue proteomes can rapidly change during tissue homogenization by the action of enzymes released from their compartments, disease specific protein species patterns can vanish. Recently, we described a novel, ultrafast and soft method for cold vaporization of tissue via desorption by impulsive vibrational excitation (DIVE) using a picosecond-infrared-laser (PIRL). Given that DIVE extraction may provide improved access to the original composition of protein species in tissues, we compared the proteome composition of tissue protein homogenates after DIVE homogenization with conventional homogenizations. A higher number of intact protein species was observed in DIVE homogenates. Due to the ultrafast transfer of proteins from tissues via gas phase into frozen condensates of the aerosols, intact protein species were exposed to a lesser extent to enzymatic degradation reactions compared with conventional protein extraction. In addition, total yield of the number of proteins is higher in DIVE homogenates, because they are very homogenous and contain almost no insoluble particles, allowing direct analysis with subsequent analytical methods without the necessity of centrifugation.

Biological significance: Enzymatic protein modifications during tissue homogenization are responsible for changes of the in-vivo protein species composition. Cold vaporization of tissues by PIRL-DIVE is comparable with taking a snapshot at the time of the laser irradiation of the dynamic changes that occur continuously under *in-vivo* conditions. At that time point all biomolecules are transferred into an aerosol, which is immediately frozen.

1. Introduction

Analysis of tissue proteome provides useful information concerning the tissue phenotype. This is of particular interest in screening for disease associated proteins, which after validation can be used as diagnostic markers for biopsy analysis. In many diseases, posttranslational modifications (PTMs) play an important role [1–3]. Due to a dysregulation of the fine-tuned protein processing machinery or pathological effects such as oxidative stress, proteins are modified, potentially leading to harmful protein species [4–7]. Therefore, to better understand disease-related proteomes on a functional level, tissue proteome must be analyzed with respect to protein species [8–10]. In the past decade, significant progress has been made in the field of proteomics that have now made protein species accessible to be studied. However, tissue homogenization is still one of the most critical and time consuming steps within a proteomic workflow. Homogenization of tissues is necessary for releasing proteins from cells and cellular compartments into stabilizing buffer solutions. The process requires the disruption of the outer cell membrane, intracellular membranes and the surrounding

* Corresponding author at: Tel.: + 04940 741058795; fax: + 04940 40097.
E-mail address: hschluet@uke.de (H. Schlüter).

http://dx.doi.org/10.1016/j.jprot.2015.12.029

extracellular structures. Here, tissue consistency defines the appropriate homogenization method [11,12]. During tissue homogenization the cell integrity is disrupted and proteins are released from the intracellular compartments resulting in proteolysis and enzymatic degradation reactions removing posttranslational protein modifications [13–15]. Although a number of methods for protease inactivation such as the addition of specific protease inhibitors, precipitation, pH adjustment, as well as heating [11,16,17] do exist, these methods do not reproducibly and effectively inhibit alteration of the proteome composition caused *in-vitro* [17,18]. This effect introduces a significant variability in tissue proteome analysis [19]. Therefore, new methods are required for tissue homogenization and protein extraction that specifically minimize *in-vitro* alterations due to enzymatic protein degradation and modification.

Recently, it was demonstrated that cold vaporization of tissues with a picosecond-infrared laser (PIRL) is possible. The wavelength of PIRL is specifically tuned to excite the OH vibration stretch band in water [20]. The soft ablation of tissue by PIRL is achieved under the conditions of desorption by impulsive excitation (DIVE) [21] in which the water molecules contained within the tissue are transferred into the gas phase in an ultrafast, explosive manner. DIVE results in intact cellular biomolecules blasting out of the sample with minimized heating or shock wave damage imposed on the tissue and biomolecules [22–25]. Kwiatkowski et al. showed that the tissue proteome is present in the condensate of the DIVE-induced tissue aerosol. Furthermore, the group demonstrated that the exact chemical composition of the DIVE ablated proteins was not changed. Even enzymatic activities were detectable in the DIVE aerosol of blood plasma [21]. Because the DIVE ablation is very fast it is hypothesized that intact protein species were exposed to a minor extent to enzymatic degradation reactions compared to classical homogenization procedure. In this study we compare the protein composition of the homogenates of DIVE ablation with those from classical tissue homogenization.

2. Materials and methods

2.1. Chemicals

Water, methanol (MeOH) and acetonitrile (ACN; all HPLC-grade) were obtained from Merck (Darmstadt, Germany). Sequence-grade trypsin and resuspension buffer was purchased from Promega (Mannheim, Germany). Any other chemicals and proteins were obtained from Sigma-Aldrich (Munich, Germany from).

2.2. Human tonsils

Human tonsils were obtained from three different patients during tonsillectomy. Immediately following the tonsillectomy, one piece of tissue from the center of the tonsil of each patient was prepared. Each sample was cut into two comparable pieces (approx. dimension: 5 mm × 5 mm and 2 mm in depth) for conventional homogenization and DIVE homogenization to provide direct comparison of identically prepared tissue. In addition, from each sample sections were used for histological staining. The pieces dedicated for further experiments were frozen in liquid nitrogen right after preparation and stored by −80 °C.

2.3. Pancreas

Pancreas was obtained from six different Wistar rats. The rats were killed in line of another experiment which was approved by the local licensing authority (Behörde für Soziales, Familie, Gesundheit, Verbraucherschutz; Amt für Gesundheit und Verbraucherschutz; Billstr. 80, D-20539 Hamburg, Germany) and supervised by the institutional animal welfare officer at the UKE. The pancreas was extracted and prepared immediately after euthanasia of the animals by carbon dioxide inhalation. Each of the six pancreas samples was prepared into 2 equal pieces of tissue. A separate tissue slice was prepared from each piece of tissue for histology. The pieces dedicated for further experiments were frozen in liquid nitrogen right after preparation and stored by −80 °C. One piece was homogenized either mechanically (MTH) and with PIRL-DIVE (DTH) to enable a direct comparison of effectively identically prepared tissue.

2.4. Histology

For histological staining tissue samples were fixed in phosphate buffered 3.5% formaldehyde. Specimens were then embedded in paraffin, cut into 4-μm thick sections, and stained with hematoxylin and eosin (H.E., Merck, Darmstadt, Germany) [26]. Stained samples were then scanned using MIRAX SCAN (Carl Zeiss Microimaging GmbH, Jena, Germany) (Supplemental Text, Figs. S1–S2).

2.5. DIVE homogenization

The PIRL (PIRL-HP2-1064 OPA-3000, Attodyne Inc. Toronto, Canada) operated at a wavelength of 3 μm, a repetition rate of 1 kHz and a pulse width of 300 ps. The PIRL beam was delivered and focused onto the sample surface with a home-built optical system. The optical power at the sample surface was approximately 450 mW. The optical energy density at the sample surface was 3.39 J/cm^2 and the average optical power density was 3.39×10^3 W/cm^2. The PIRL beam was scanned at the speed of 130 mm/s during the ablation process. Frozen human tonsil tissue was placed in a home-built ablation chamber equipped with a funnel, which was connected with a wash-bottle within a cryo-trap. For homogenization tissues with a dimension of approximately 5 mm × 5 mm and 2 mm in depth were irradiated with PIRL. The DIVE ablation plume was captured inside the wash-bottle (condensate of the DIVE aerosol, DIVE homogenate, DH).

2.6. DIVE homogenization of human tonsils and protein extraction

In case of human tonsil experiments the wash bottle was filled with a powder of urea (m = 210.21 mg), thiourea (m = 76.12 mg) and Tris–HCl (m = 1.82 mg). The DIVE condensates were thawed and adjusted to a total volume of 500 μL with HPLC-H_2O and 1.23 μL 2-hydroxyethyl disulfide (HED) resulting in a concentration of 7 M urea, 2 M thiourea, 30 mM Tris–HCl and 20 mM HED (DIVE homogenate, DH). DIVE homogenates were incubated for 1 h at room temperature. After incubation, samples were centrifuged at 15,000 ×*g* for 5 min. The supernatants were transferred into a 2 mL reaction vial. Proteins were precipitated and protein concentrations were determined using the 2-D Quant Kit (GE Healthcare Life Sciences, Freiburg, Germany) following the manufacturer's instruction. For each sample 200 μg was used for two dimensional gel electrophoresis and 40 μg was used for SDS-PAGE.

2.7. DIVE homogenization of rat pancreas and protein extraction

For homogenization of rat pancreas tissue samples the DIVE ablation plume was captured in a wash-bottle. The frozen condensates were thawed with 100 μL five times concentrated Laemmli buffer (0.225 M Tris–HCl, pH 6.8; 50% glycerol; 5% SDS; 0.05% bromophenol blue; 0.25 M DTT, T = 95 °C) and immediately transferred in a boiling water bath. The volume was adjusted with MS-H_2O to 500 μL and the DIVE homogenates were incubated in the boiling water bath for 5 min. DIVE homogenates were centrifuged at 15,000 ×*g* for 3 min. The supernatants were transferred into a 2 mL reaction vial. Protein concentration of the condensates was determined using 2-D Quant Kit (GE Healthcare Life Sciences, Freiburg, Germany) following the manufacturer's instruction. For each sample 30 μg was loaded on SDS-PAGE.

2.8. DIVE homogenization of rat pancreas spiked with alpha-casein

For spiking experiments rat pancreas tissue samples were ablated and the ablation products were captured in a wash-bottle filled with a powder of urea (m = 210.21 mg), thiourea (m = 76.12 mg) and Tris–HCl (m = 1.82 mg) and 180 μg alpha-Casein (c = 1.8 μg/μL, dissolved in HPLC-H_2O). The DIVE condensates were thawed and adjusted to a total volume of 500 μL with HPLC-H_2O resulting in a concentration of 7 M urea, 2 M thiourea, 30 mM Tris–HCl (pH 6.8). DIVE homogenates of rat pancreas were centrifuged at 15,000 ×*g* for 3 min. The supernatants were transferred into a 2 mL reaction vial. Protein concentration of the condensates was determined using 2-D Quant Kit (GE Healthcare Life Sciences, Freiburg, Germany) following the manufacturer's instruction. For each sample 30 μg was loaded on SDS-PAGE.

2.9. Mechanical homogenization

2.9.1. Mechanical homogenization of human tonsils and protein extraction

For conventional mechanical tissue homogenization a human tonsil tissues with a dimension of approximately 5 mm × 5 mm and 2 mm were lyophilized for 24 h. The lyophilized and frozen tissues were grinded with a cryo-grinder in the presence of liquid nitrogen. The mechanical homogenates (MH) were dissolved in 500 μL lysis buffer (7 M urea, 2 M thiourea, 30 mM Tris–HCl, 20 mM HED, dissolved in HPLC-H_2O). Mechanical homogenates were incubated for 1 h at room temperature. After incubation, samples were centrifuged at 15,000 ×*g* for 5 min. The supernatants were transferred into a 2 mL reaction vial. Proteins were precipitated and protein concentrations were determined using the 2-D Quant Kit (GE Healthcare Life Sciences, Freiburg, Germany) following the manufacturer's instruction. For each sample 200 μg was used for two dimensional gel electrophoresis and 40 μg was used for SDS-PAGE.

2.9.2. Mechanical homogenization of rat pancreas and protein extraction

Frozen rat pancreas tissue samples were homogenized in the presence of 500 μL lysis buffer (45 mM M Tris–HCl, pH 6.8; 10% glycerol; 1% SDS; 0.01% bromophenol blue; 0.05 M DTT) using a bead mill (TissueLyser II, Quiagen, Hamburg, Germany) with a 3 mm stainless steel bead (time: 3.3 min, frequency: 25/s). Mechanical homogenates of rat pancreas were centrifuged at 15,000 ×*g* for 3 min. The supernatants were transferred into a 2 mL reaction vial. Protein concentration of the condensates was determined using 2-D Quant Kit (GE Healthcare Life Sciences, Freiburg, Germany) following the manufacturer's instruction. For each sample 30 μg was loaded on SDS-PAGE.

2.9.3. Mechanical homogenization of rat pancreas spiked with alpha-casein

Frozen rat pancreas tissue samples were homogenized in the presence of 500 μL lysis buffer (7 M urea, 2 M thiourea, 30 mM Tris–HCl, pH 6.8) containing 180 μg alpha-casein using a bead mill (TissueLyser II, Quiagen, Hamburg, Germany) with a 3 mm stainless steel bead (time: 3.3 min, frequency: 25/s). Mechanical homogenates were centrifuged at 15,000 ×*g* for 3 min. The supernatants were transferred into a 2 mL reaction vial. Protein concentration of the condensates was determined using 2-D Quant Kit (GE Healthcare Life Sciences, Freiburg, Germany) following the manufacturer's instruction. For each sample 30 μg was loaded on SDS-PAGE.

2.9.4. Two dimensional gel electrophoresis

Two dimensional electrophoresis (2DE) was performed by Proteome Factory AG based on the protocol by Klose and Kobalz [27]. Isoelectric focusing (first dimension) was made in vertical rod gels containing 9 M urea, 4% acrylamide, 0.3% piperazine diacrylamide, 5% glycerine, 2% carrier ampholyte (pH 2–11), 0.06% TEMED, and 0.08% ammonium persulfate. For each sample 200 μg of the protein extract was focused at 8820 Vh. SDS-PAGE (second dimension) was performed in gels (0.1 cm, 20 cm, 30 cm; 15% acrylamide, 0.2% bisacrylamide, 375 mM Tris–HCl (pH 8.8), 0.1% SDS, 0.03% TEMED, and 0.08% ammonium persulfate). 2DE gels were stained with FireSilver (Proteome Factory, Berlin, Germany).

2.9.5. Image analysis

Images of 2D gels were analysed using Delta2D (version 4.4; Decodon, Greifswald, Germany) according to instructions based on Berth et al. [28]. In brief, images of the 2D gels of the DIVE homogenate (DH) and the conventional, mechanical homogenate (MH) of every biological sample was warped against each other to correct positional spot variations. The gel images were fused to generate the proteome map containing the information of all protein spots for each biological sample. Spot detection was performed on the proteome map and a consensus spot pattern was applied to the DH and the MH gels. Comparison was performed on the basis of the spot intensities. Spots specific for one of the homogenization methods were identified according to the intensity ratio between DH and MH.

2.9.6. One dimensional gel electrophoresis

The samples were dissolved in 5 μL 4× sample buffer (XT sample buffer, Bio-Rad, Munich, Germany), 1 μL 20× reducing agent (XT reducing agent, Bio-Rad, Munich, Germany) and filled up to 20 μL with HPLC-grade water. The samples were incubated at 95 °C for 5 min and loaded onto a 10% Criterion™ XT Bis-Tris gel (Bio-Rad, Munich, Germany). Proteins were separated at a constant voltage of 120 V for 45 min. The gel was stained for 2 h with a Coomassie solution (40% MeOH, 10% acetic acid, 0.025% Coomassie blue-250, dissolved in H_2O) and destained with 40% MeOH. For tryptic in-gel digest the SDS-PAGE lanes of the DIVE homogenate (DH) and the conventional, mechanical homogenate (MH) were cut in comparable bands.

2.9.7. Tryptic in-gel digestion

In-gel digestion was performed in accordance with Shevchenko et al. [29]. Briefly, shrinking and swelling was achieved with pure ACN and 100 mM NH_4HCO_3. For in-gel reduction 10 mM dithiothreitol (dissolved in 100 mM NH_4HCO_3) was used and alkylation was achieved with 55 mM iodacetamide (dissolved in 100 mM NH_4HCO_3). For trypsin digestion the gel pieces were covered with a trypsin solution (13 ng/μL sequencing-grade trypsin, dissolved in 10 mM NH_4HCO_3 containing 10% ACN) and incubated at 37 °C for 12 h. Tryptic peptides were extracted with 5% FA, 50% ACN and evaporated. For further LC–MS/MS analysis, samples were dissolved in 20 μL 0.1% FA.

2.9.8. LC–MS/MS analysis

LC–MS/MS measurements were performed by injecting the samples on a nano liquid chromatography system (Dionex UltiMate 3000 RSLCnano, Thermo Scientific, Bremen, Germany) coupled via electrospray-ionization (ESI) to a linear trap quadrupole (LTQ) orbitrap mass spectrometer (Orbitrap Fusion, Thermo Scientific, Bremen, Germany) or with nano liquid chromatography system (nanoACQUITYy, Waters, Manchester, UK) coupled via ESI to a quadrupole orbitrap mass spectrometer (Orbitrap QExcactive, Thermo Scientific, Bremen, Germany). The samples were loaded (5 μL/min) on a trapping column (Acclaim PepMap μ-precolumn, C18, 300 μm × 5 mm, 5 μm, 100 Å, Thermo Scientific, Bremen, Germany; nanoACQUITY UPLC Symmetry C18 trap column, 180 μm × 20 mm, 5 μm, 100 Å; buffer A: 0.1% FA in HPLC-H_2O; buffer B: 0.1% FA in ACN) with 2% buffer B. After sample loading the trapping column was washed for 5 min with 2% buffer B (5 μL/min) and the peptides were eluted (200 nL/min) onto the separation column (Acclaim PepMap 100, C18, 75 μm × 250 mm, 2 μm, 100 Å, Thermo Scientific, Bremen, Germany; nanoAcquity UPLC column, BEH 130 C18, Waters; 75 μm × 250 mm, 1.7 μm, 100 Å; 200 nL/min, gradient: 2–30% B in 30 min). The spray was generated from a fused-silica emitter (I.D. 10 μm, New Objective, Woburn, USA) at a capillary voltage of 1650 V. Mass spectrometric analysis was performed in positive ion mode. LC–MS/MS analysis with orbitrap Fusion was carried out in data dependant

acquisition mode (DDA) using top speed mode, a HCD collision energy of 28%, an intensity threshold of 2e5 and an isolation width of 1.6 m/z. Every second a MS scan was performed over a m/z range from 400 to 1500, with a resolution of 120,000 FWHM at m/z 200 (transient length = 256 ms, maximum injection time = 50 ms, AGC target = 2e5). MS/MS spectra were recorded in the ion trap (scan-rate = 66 kDa/s, maximum injection time = 200 ms, AGC target = 1e4). LC–MS/MS analysis with the orbitrap QExcactive was performed on MS level over a m/z range from 400 to 1500, with a resolution of 70,000 FWHM at m/z 200 (transient length = 256 ms, injection time = 100 ms, AGC target = 3e6). MS/MS measurements were carried out using in DDA mode (Top5), with a HCD collision energy of 30%, a resolution of 17,000 FWHM at m/z 200 (transient length = 64 ms, injection time = 100 ms, AGC target = 3e6), an underfill ratio of 10% and an isolation width of 2 m/z.

2.9.9. Data analysis

LC–MS raw data from the 2DE spots were processed with Proteome Discoverer 2.0 (Thermo Scientific, Bremen, Germany). For identification MS/MS spectra were searched with Sequest HT against the human SwissProt database (www.uniprot.org, downloaded November 10, 2014, 20,161 entries) and a contaminant database (298 entries). The searches were performed using the following parameters: precursor mass tolerance was set to 10 ppm and fragment mass tolerance was set to 0.5 Da. Furthermore, two missed cleavages were allowed and a carbamidomethylation on cysteine residues as a fixed modification as well as an oxidation of methionine residues as a variable modification. Peptides were identified with a FDR of 1% using Percolator. Proteins were kept as correctly identified if at least two unique peptides were identified.

LC–MS raw data from the SDS-PAGE bands were processed with MaxQuant (version 1.5.2.8) [30]. Peptide and protein identification was carried out with Andromeda against a human and a contaminant database as described above in case of the human tonsil and against a SwissProt database of *Rattus norvegicus* (www.uniprot.org, downloaded November 10, 2015, 7940 entries; spiked with protein sequences of bovine alpha-S1/S2-casein in case of spiking experiments). The searches were performed using the following parameters: precursor mass tolerance was set to 10 ppm and fragment mass tolerance was set to 0.5 Da for orbitrap Fusion measurements and to 20 ppm for orbitrap QExcactive measurements. For peptide identification two miss cleavages were allowed, a carbamidomethylation on cysteine residues as static modification and an oxidation of methionine residues as a variable modification. For spiking experiments a phosphorylation on serine residues was also taken into account. Peptides and proteins were identified with a FDR of 1%. For a protein identification at least two of its unique peptides had to be detected.

Proteins were quantified with the MaxLFQ algorithm [31] considering only unique peptides and a minimum ratio count of three. Protein species migration profiles of the SDS-PAGE of the DIVE homogenate and the mechanical homogenate were generated by applying the label-free quantification (LFQ) intensities of the proteins to the corresponding band on the SDS-PAGE (Fig. S3).

For global analysis of proteolysis a comparison of the migration profiles of the proteins was performed. For each protein, a migration profile was created from the LFQ intensities in the bands of the SDS gel. Migration profiles were smoothed with a Gaussian filter with a radius of 2 and the position of the highest signal (migration peak) was determined for both homogenization methods. Histograms of the relative migration peak shifts between mechanical and DIVE homogenization were created from of all proteins that were detected in both homogenization methods with a non-zero LFQ intensity to estimate the difference in the overall degree of proteolysis (Figs. S18–S23). Proteins which were shifted towards lower molecular weights in the SDS-PAGE by at least two bands were considered proteolysed (Fig. S3). An enrichment analysis of the shifted proteins was performed with DAVID [32,33]. The subsets of the shifted proteins were compared with the background of proteins that were present in both homogenization methods. The functional annotation chart tool was used with the gene ontology (GO) cellular component database.

3. Results and discussion

To investigate the hypothesis that intact protein species undergo less enzymatic degradation due to minor exposure to enzymatic reactions during DIVE homogenization compared with classical homogenization, human tonsillar tissue samples were homogenized by either DIVE (DIVE homogenate, DH) or with a mechanical cryo-grinder (mechanical homogenate, MH). From both homogenates equal amounts of proteins (m = 200 μg) were applied to high-resolution two dimensional gel electrophoresis (2DE, Fig. 1, Fig. S4, Scheme 1). Image analysis of the 2DE-protein patterns revealed that on average 719 spots were present on both gels, 110 spots (15.3%) were only present on the 2DE-gel of MH and 107 spots (14.9%) were only detected on the 2DE-gel of DH (Fig. S5, Table S1). On average 67 (66.7%) of the 110 spots only detected on the gel of the MH had molecular weights less than 32 kDa, whereas 92 (86.3%) of the 107 spots, which were only detected on the gel of the DH had a molecular weight higher than 32 kDa. The average number of spot chains detected on the MH-2DE gels was 14 and 18 for the DH-2DE gels.

The 2DE-protein patterns of both homogenates showed similarities as well as significant differences (Fig 1, Table 1). The smear on DH-2DE gel may be explained by decreased loss of lipids, which were getting lost during MTH and therefore less smear was observed on MH-2DE gel. Most obvious was the difference in the molecular weight range from 30 kDa to 58 kDa and between the isoelectric points pH 7.5 and pH 9 (Fig. 1, marked with a rectangle). In the enlarged areas of these rectangles four spots are present in both gels (Fig. 1, MH spot no.*9–*12, DH 9–12). The spots were identified by LC–MS/MS (Table 1, Supporting Information 1 (MH), Supporting Information 2 (DH)) as pyruvate kinase PKM (spot no.*9 (MH), 9 (DH)), annexin A2 (spot no.*10 (MH), 10 (DH)), L-lactate dehydrogenase A chain (spot no.*11 (MH), 11 (DH)) and voltage dependent anion-selective channel protein 1 (spot no.*12 (MH), 12 (DH)). A number of spots and spot chains were present next to these four protein spots on the 2DE gel of the DH, which were missing on the gel of the MH (Fig. 1). The spot chain consisting of spot no. 13–22 (Fig. 1, DH) was attributed to protein species of glyceraldehyde-3-phosphate dehydrogenase (Table 1). Additional protein species of glyceraldehyde-3-phosphate dehydrogenase was also identified in spot no. 26. In total, eleven glyceraldehyde-3-phosphate dehydrogenase species were identified on the 2DE gel of the DH. Glyceraldehyde-3-phosphate dehydrogenase is known as a protein with several phosphorylation and acetylation sites [34–36]. In contrast, only one spot (Fig. 1, MH spot no. *13) was identified as glyceraldehyde-3-phosphate dehydrogenase in the corresponding section of the 2DE gel of the MH.

The 2DE gel of the MH showed six intense spots between pH 6 and pH 9 at a molecular weight less than 20 kDa (Fig. 1, MH spot no. *1–*8). The LC–MS/MS analysis revealed that the spots were caused by protein species of hemoglobin subunit alpha (HBA, Mr. = 15.2 kDa, spot no. *6 & *7), hemoglobin subunit beta (HBB, Mr. = 16 kDa, spot no. *1–*5 and *8), hemoglobin subunit delta (HBD, Mr. = 16 kDa, spot no. *2–*5 and *8) and profilin (Mr = 15 kDa, spot no. *1 & *4). In spot no. *7 and *8 protein species of HBA, HBB and HBD were identified with a molecular weight less than 10 kDa. Together with the identification of myosin protein species (Mr = 222 kDa) in spot no. *6, next to intact HBA species, these findings indicated a proteolytical protein degradation during the sample preparation. The 2DE gel of the DH showed in the corresponding part of the gel six intense spots (Fig. 1, DH spot no. 1–6). In these spots five HBB protein species (spot no. 1–5), four HBD protein species (spot no. 2–5), two profilin-1 protein species (spot no. 1 & 4) and HBA (spot no. 6) were present. For HBA and

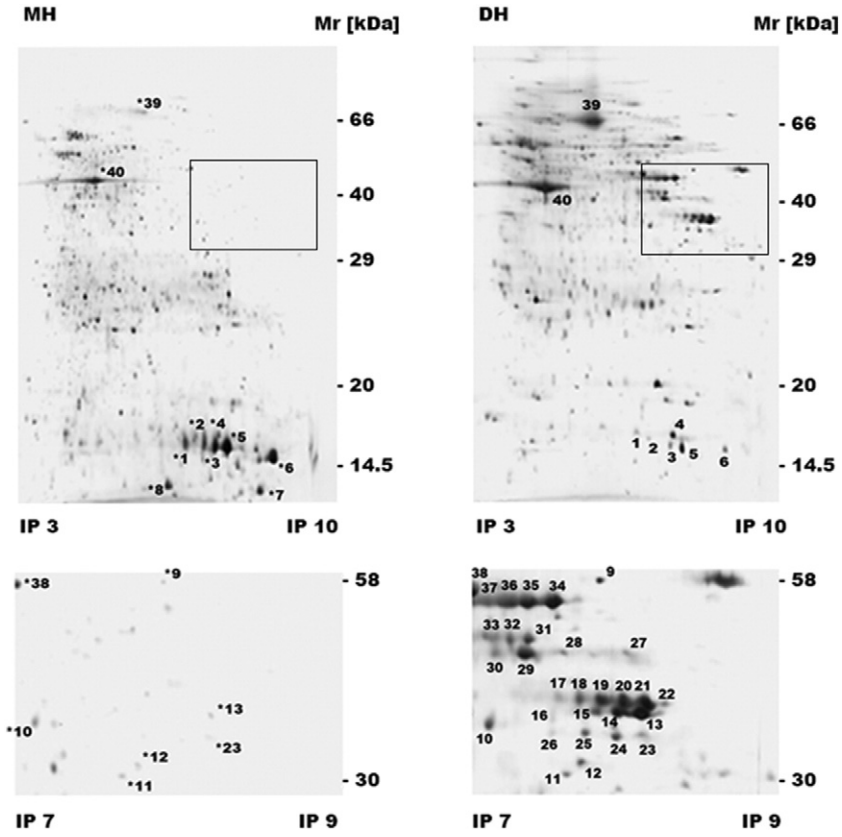

Fig. 1. Two dimensional gel electrophoresis (2DE) of protein homogenates from human tonsils no. 1. MH: 2DE of the mechanical homogenate (MH) of human tonsils (m = 200 μg). DH: 2DE of the DIVE homogenate (DH) of human tonsils (m = 200 μg). Spots identified by LC–MS/MS and described in the text, Table 1 and in supplemental results are marked with a number (DH) or with an asterisk and a number (MH).

HBB no protein species were identified that would indicate proteolysis during the sample preparation in case of DH.

In summary, the results from 2DE analysis demonstrate that by using DIVE for tissue homogenization (DTH, DIVE tissue homogenization) a higher number of protein species are conserved as compared to conventional mechanical tissue homogenization (MTH, mechanical tissue homogenization). One possible reason may be that during MTH protein species are exposed to a higher extent to enzymatic reactions resulting in a lower number of species detected from one gene. Obviously, during MTH a larger number of intact protein species are degraded by proteolysis compared to DTH. Furthermore, DH was almost completely free of particles like cell debris compared to MH. These had to be removed from the MH by centrifugation prior to 2DE and SDS-PAGE. During this process protein species may be lost through adsorption on the surface of the particles, which were removed by centrifugation [37].

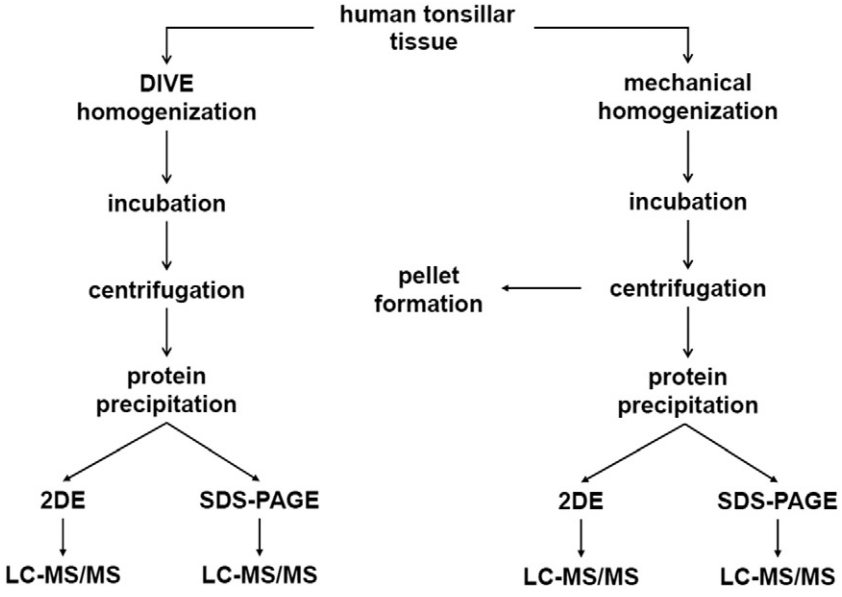

Scheme 1. Experimental work-flow.

Table 1
Proteins identified in selected spots of the 2DE gel (Fig. 1) of the DIVE homogenate (DH) and the mechanical homogenate (MH). X: spot was not present.

Protein	Spot no. DH	Spot no. MH
Hemoglobin subunit alpha OS = *Homo sapiens* GN = HBA PE = 1 SV = 2	6	*6, *7
Hemoglobin subunit beta OS = *Homo sapiens* GN = HBB PE = 1 SV = 2	1–5	*1–*5; *8
Hemoglobin subunit delta OS = *Homo sapiens* GN = HBD PE = 1 SV = 2	2–3, 5	*2–*3, *5
Profilin-1 OS = *Homo sapiens* GN = PFN1 PE = 1 SV = 2	1, 4	*1, *4
Myosin-7 OS = *Homo sapiens* GN = MYH7 PE = 1 SV = 5	X	*6
Myosin-1 OS = *Homo sapiens* GN = MYH1 PE = 1 SV = 3	X	*6
Myosin-2 OS = *Homo sapiens* GN = MYH2 PE = 1 SV = 1	X	*6
Myosin-4 OS = *Homo sapiens* GN = MYH4 PE = 1 SV = 2	X	*6
Pyruvate kinase PKM OS = *Homo sapiens* GN = PKM PE = 1 SV = 4	9	*9
Annexin A2 OS = *Homo sapiens* GN = ANXA2 PE = 1 SV = 2	10	*10
Voltage-dependent anion-selective channel protein 1 OS = *Homo sapiens* GN = VDAC1 PE = 1 SV = 2	11	*11
i-lactate dehydrogenase A chain OS = *Homo sapiens* GN = LDHA PE = 1 SV = 2	12	*12
Glyceraldehyde-3-phosphate dehydrogenase OS = *Homo* sapiens GN = GAPDH PE = 1 SV = 3	13-22	*13
Heterogeneous nuclear ribonucleoproteins A2/B1 OS = *Homo sapiens* GN = HNRNPA2B1 PE = 1 SV = 2	22-25	*23
Malate dehydrogenase, mitochondrial OS = *Homo sapiens* GN = MDH2 PE = 1 SV = 3	23-24	*23
Fructose-bisphosphate aldolase A OS = *Homo sapiens* GN = ALDOA PE = 1 SV = 2	27	X
Phosphoglycerate kinase 1 OS = *Homo sapiens* GN = PGK1 PE = 1 SV = 3	28-31	X
Elongation factor Tu, mitochondrial OS = *Homo sapiens* GN = TUFM PE = 1 SV = 2	32-33	X
Actin, aortic smooth muscle OS = *Homo sapiens* GN = ACTA2 PE = 1 SV = 1	33	X
Alpha-enolase OS = *Homo sapiens* GN = ENO1 PE = 1 SV = 2	34-38	X
Beta-enolase OS = *Homo sapiens* GN = ENO3 PE = 1 SV = 5	34-38	*38
Gamma-enolase OS = *Homo sapiens* GN = ENO2 PE = 1 SV = 3	34	X
Serum albumin OS = *Homo sapiens* GN = ALB PE = 1 SV = 2	39	*39
Actin, alpha skeletal muscle OS = *Homo sapiens* GN = ACTA1 PE = 1 SV = 1	40	40
Actin, alpha cardiac muscle 1 OS = *Homo sapiens* GN = ACTC1 PE = 1 SV = 1	40	40
Actin, aortic smooth muscle OS = *Homo sapiens* GN = ACTA2 PE = 1 SV = 1	40	40
Actin, gamma-enteric smooth muscle OS = *Homo sapiens* GN = ACTG2 PE = 1 SV = 1	40	40

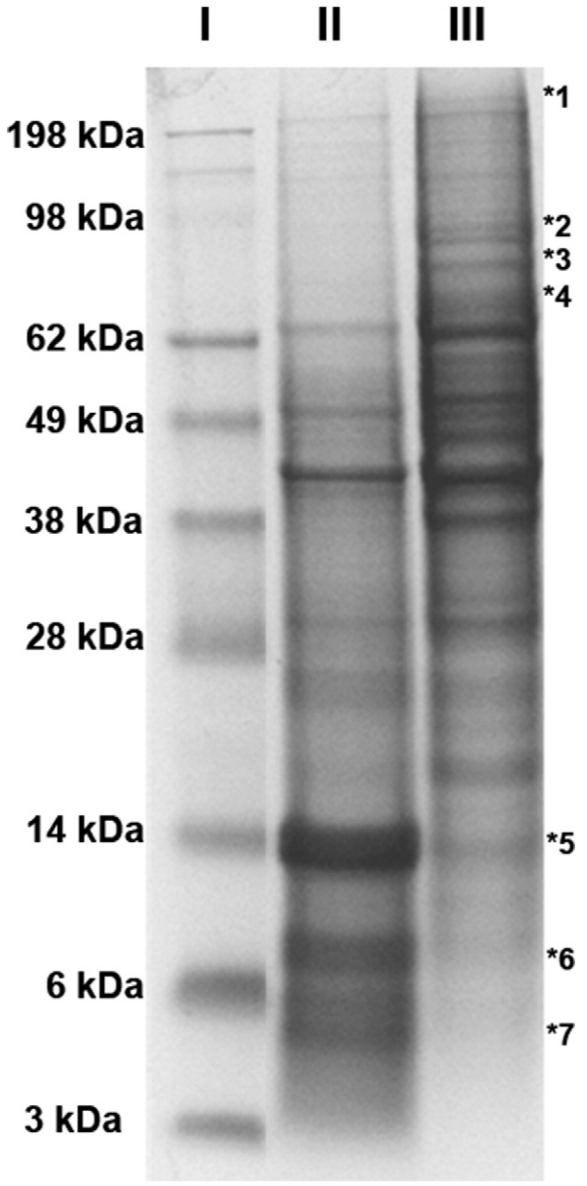

Fig. 2. SDS-PAGE of protein homogenates from human tonsil no. 1. I: protein marker. II: Protein sample of human tonsils yielded by mechanical homogenization (MH, m = 40 μg). III. Protein sample of human tonsils yielded by DIVE homogenization (DH, m = 40 μg). Bands described in the text and in the supplemental results (Figs. S6, S7, S13–S16) are marked with an asterisk and a number.

A difference in the distribution of abundant proteins was also evident between the 2DE protein patterns (Fig. 1) of DH and MH. In the latter, the spots of the diverse protein species of hemoglobin are the most abundant proteins (Fig. 1, MH, spots *1–*7. In DH glyceraldehyde-3-phosphate dehydrogenase (Fig. 1, DH, spots 13–22 & 26) beta-enolase (Fig. 1, DH, spots 34–38), albumin (Fig. 1, DH, spot 39) and actin proteins (Fig. 1, DH, spot 40) are the most abundant protein species. In addition to the different time-scales on which intact protein species were exposed to enzymatic degradation reaction during DTH and MTH, the difference in sample preparation following DTH and MTH may be responsible for this observation as described above.

In order to further investigate if DIVE tissue homogenates are associated with less proteolysis, equal amounts of proteins from DH and MH were subjected to SDS-PAGE (Fig. 2 Fig. S24, Scheme 1). A comparison of the intensity of the bands of the MH- and DH-SDS-PAGE lanes showed that many bands larger than 14 kDa were more intense in DH samples and that the overall number of bands was larger than in the lanes of the MH samples. In the SDS-PAGE of the MH sample bands smaller than 14 kDa were notably more intense than in the SDS-PAGE of the DH sample. The difference in the distribution of abundant proteins was in good accordance with the results of the 2DE analysis. As described above, the difference in sample preparation following DTH and MTH as well as different exposure times to enzymatic degradation reactions may be responsible for the different distribution of abundant protein bands on the SDS-PAGE gels. It was assumed as a rough estimation that in the DH intact protein species were exposed to enzymatic degradation reactions to a lesser extent. Further, for tryptic in-gel digestion, both MH- and DH-SDS-PAGE lanes were cut in comparable bands (Fig. S25) and subjected to qualitative and quantitative protein analysis. The resulting data were used for relative quantification of the corresponding proteins and to construct SDS-PAGE-migration profiles. Since separation in the first dimension was performed on intact protein level according to the size of the protein species, the correlation between the identified tryptic peptides and the molecular mass of the corresponding protein species before tryptic digestion is given. SDS-PAGE-migration profiles represent the distribution of protein species coded by one single gene occurring with different molecular masses. If

intact protein species are degraded during sample preparation, new protein species with lower molecular masses are generated thus appearing in the migration profiles at lower molecular masses. Based on the SDS-PAGE-migration profiles (Fig. S3) and the SDS-PAGE-migration shift peak histograms (Figs. S18–S20) the global degree of proteolysis between MH and DH was estimated. The observed degree of proteolysis was on average significantly lower in case of DTH (2.33% (+/− 0.58%)) compare to MTH (23.33% (+/− 11.02%)) (Fig. 4D, Figs. S18–S20). An enrichment analysis revealed an overrepresentation of proteins from ribosomal complexes and cell organelles among the proteins shifted towards lower molecular weight after MTH (Fig. S26). In addition, the degree of proteolysis was compared by determining the number of semi-tryptic peptides in DH and MH in the presence and absence of chymotryptic peptides. The results (data not shown) confirmed those obtained from the SDS-migration profiles and migration shift peak histograms. However, the latter two results were more clear.

The different degrees of enzymatic degradation between MH and DH were especially obvious for the protein collagen alpha-3(VI) chain (Fig. 2, *1) and Ku70 (Fig. 2, *4). Collagen alpha-3(VI) chain (Mr = 343.7 kDa) was identified as the main component in the band underneath the loading pocket of the DH sample (Fig. 2, *1), whereas this protein species was not identified in the corresponding area in the SDS-PAGE of MH. The SDS-PAGE-migration profile of collagen alpha-3(VI) chain of DH showed that the identified collagen alpha-3(VI) chain species were almost entirely confined to the molecular range above 200 kDa (Fig. 3), whereas the SDS-PAGE-migration profile of MH revealed a number of different collagen alpha-3(VI) chain protein species, that were presumably created by proteolytical degradation. The proteolysis species of collagen alpha-3(VI) chain were detected over the entire SDS-PAGE covering a molecular range from 100 kDa down to 3 kDa (Fig. 3, Fig. S9). This result indicates a high degree of collagen alpha-3(VI) chain proteolysis during sample preparation in case of MTH, which was not observed with the DIVE approach. Collagen degradation can occur very rapidly due to a variety of proteases that are still active during tissue homogenization [38]. Since mechanical homogenization in the presence of liquid nitrogen of the lyophilized tissue lasts several minutes, collagen proteins can be significantly degraded by proteases. In contrast, DIVE transfers proteins on a millisecond time-scale from tissues into a liquid homogenate thus reducing total time intact collagen species were exposed to proteases.

Similar results were obtained for the DNA repair protein Ku70 (XRCC6, Mr. = 69.9 kDa, Fig. 2, *4). The SDS-PAGE-migration profile revealed that almost only intact protein species of the Ku70 gene were identified in DH (Fig. 3, Fig. S17). While the intact Ku70 protein species could not be identified in the SDS-PAGE from MH (Fig. 3, Fig. S17). However, Ku70 was identified in high quantities between 26 kDa and 14 kDa as well as down to at least 3 kDa (Fig. 3). The results for Ku70 indicated that intact protein species were completely degraded by proteases. Since the DH-SDS-PAGE showed almost exclusively the intact Ku70 species and no degradation products, it was assumed that in DH a higher number of intact Ku70 species were identified due to the fast transfer of the intact species from the tissue into the condensate, whereby the time for proteolytical reactions was reduced during sample preparation.

The intense stained band in the SDS-PAGE of the MH next to the 14 kDa marker band (Fig. 2, *5) contained HBA, HBB and HBD as the main proteins. Different protein species of HBA, HBB and HBD were also identified as the major components of the two bands slightly above and under the 6 kDa marker band (Fig. 2, *6, *7). The SDS-PAGE of the DH shows a band next to the 14 kDa marker band as well, which was caused by HBA, HBB and HBD. In contrast to the MH-SDS-PAGE, the 10-kDa-heat-shock-protein was identified as the major component in the faint band slightly above the 6 kDa marker band. The SDS-PAGE-migration profiles of HBA, HBB and HBD (Figs. S8, S10–S12) revealed for DH an almost exclusive detection of HBA, HBB and HBD at approximately 14 kDa, whereas for MH species of HBA, HBB and HBD were not only detected at approximately 14 kDa, but also at molecular weights lower than 10 kDa. These results confirmed the observation of the 2DE-analysis, indicating proteolytical degradation of HBA, HBB and HBD during sample preparation, which was not observed using DIVE for tissue homogenization.

A comparison of the number of proteins identified by LC–MS/MS analysis of the SDS-PAGE of the three biological tonsil replicates showed that DTH resulted in a higher number of identified proteins compared to MTH (Fig. 4 A; DTH: 2085 proteins (+/− 366), MTH: 1850 proteins (+/− 667)). In addition a considerably higher number of proteins (1343 proteins, Fig. 4B) were identified in all three replicates using DTH compared to MTH (974 proteins, Fig. 4B). Of these proteins 839

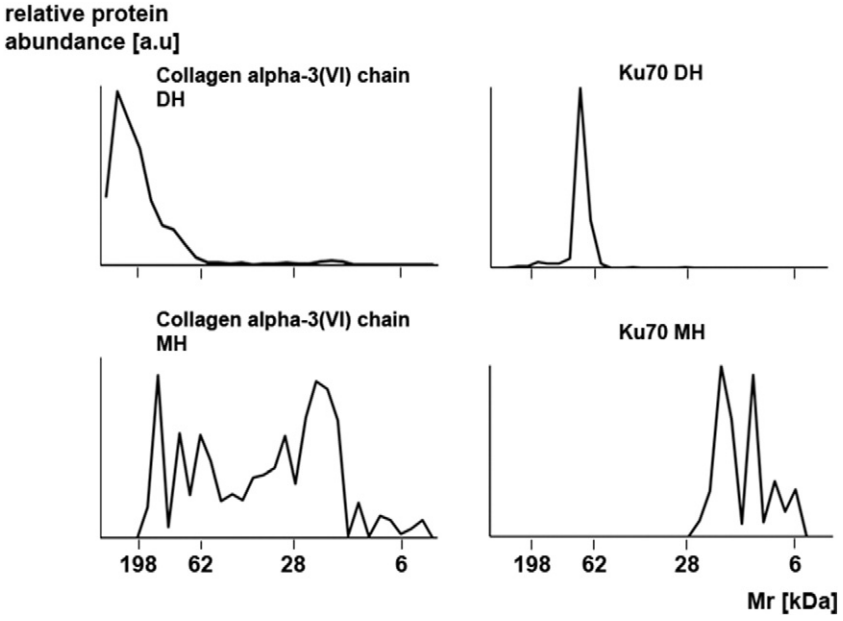

Fig. 3. SDS-PAGE-migration profiles of collagen alpha-3(VI) chain species and DNA repair protein Ku70 species, constructed from the relative quantities of their species, identified by tryptic digestion and subsequent LC–MS/MS analysis in the individual SDS-PAGE bands of the lanes of the protein extracts from human tonsils yielded by mechanical homogenization (MH) and DIVE homogenization (DH).

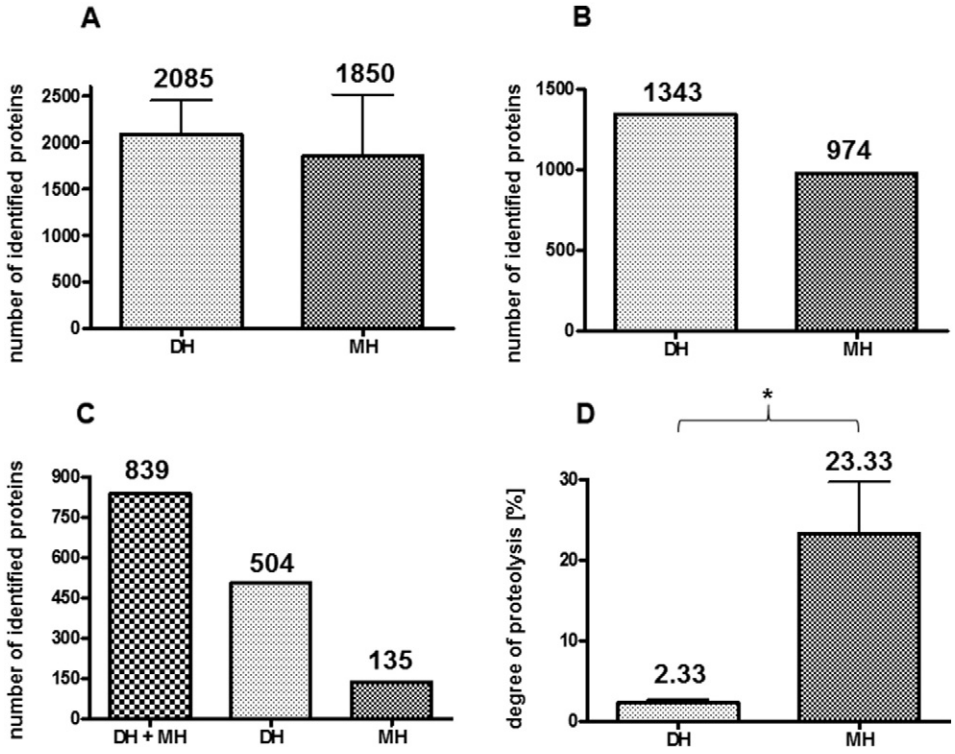

Fig. 4. Statistical analysis of the LC–MS/MS data from the SDS-PAGE of the DIVE homogenates (DH) and the mechanical homogenates (MH) from human tonsils (n = 3). A: Histogram (mean with standard deviation (SD)) showing the total number of proteins identified in the three biological replicates. B: Histogram of the number of proteins identified in all three biological replicates. C: Histogram showing the number of proteins identified in all three biological replicates in both DH and MH, only in DH and only in MH. D: Histogram (mean with SD) showing the global degree of proteolysis in the three biological replicates, *: p = 0.03 (t-test). At least two unique peptides had to be identified for a protein to be taken into account.

(56.8%) were identified in both DTH and MTH. Although 134 proteins (9.1%) were only identified in MH, a considerably higher number of proteins (504 proteins, 34.1%) were exclusively identified in DH. This result shows that by using DIVE for tissue homogenization a considerably higher number of proteins was identified as compared to the mechanical homogenization. Alltogether, the number of identified

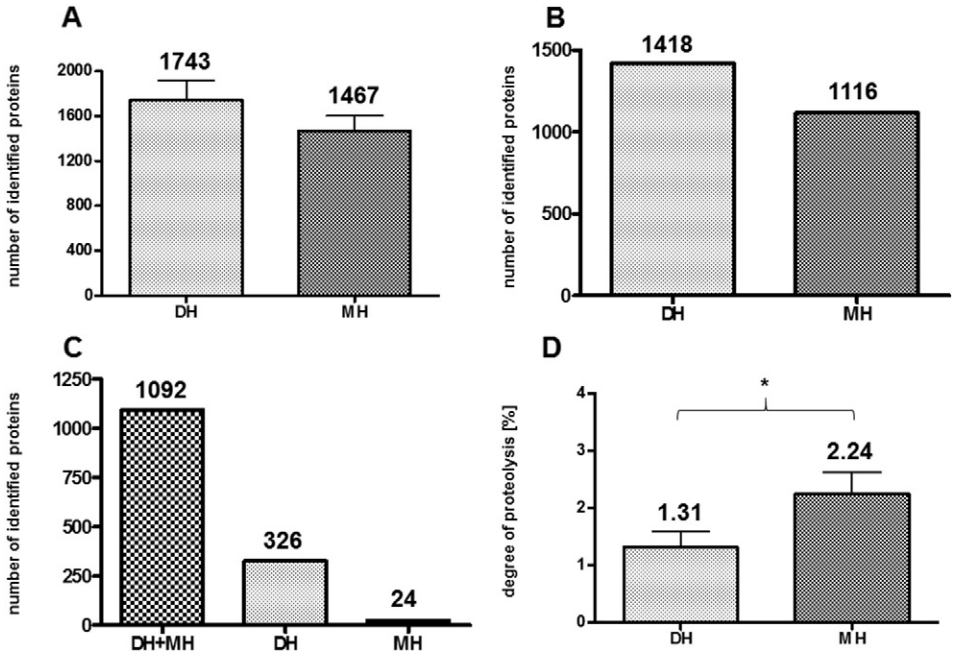

Fig. 5. Statistical analysis of the LC–MS/MS data from the SDS-PAGE of the DIVE homogenates (DH) and the mechanical homogenates (MH) from rat pancreas (n = 3). A: Histogram (mean with standard deviation (SD)) showing the total number of proteins identified in the three biological replicates. B: Histogram of the number of proteins identified in all three biological replicates. C: Histogram showing the number of proteins identified in all three biological replicates in both DH and MH, only in DH and only in MH. D: Histogram (mean with SD) showing the global degree of proteolysis in the three biological replicates, *: p = 0.0277 (t-test). At least two unique peptides had to be identified for a protein to be taken into account.

proteins are lower compared to other proteomics studies recently published, since rather strict parameters were used for both data acquisition and protein identification as described in the materials and methods section.

In addition, pancreas tissue samples from rat were homogenized either by DIVE ablation (DTH) or mechanical using a bead mill (MTH, Fig. S27). The bead mill homogenization in addition to the lyophilization-based homogenization was used since it is a common sample preparation method in proteomics. Pancreas tissue was chosen because it contains many proteases, which can be critical during sample preparation. For minimizing enzymatic degradation, the bead mill homogenates were lysed in Laemmli buffer. Hot Laemmli buffer was also added to the frozen DIVE homogenate. Immediately after addition of the buffer, the homogenates were heated in a boiling water bath for ensuring a minimum of enzymatic activities. Equal amounts of DH and MH homogenate were subjected to SDS-PAGE, followed by tryptic in-gel digestion and quantitative LC–MS/MS analysis. Global proteolysis analysis revealed that with both homogenization methods almost only intact protein species were identified. The Laemmli buffer in combination with the heating step can be assumed to be responsible for the low degree of proteolysis. However, again the average degree of proteolysis was significantly lower in case of DH (1.31% (+/− 0.27%)) than in case of MH (2.24% (+/− 0.38%)) (Fig. 5 D, Figs. S21–S23). Laemmli buffer in combination with sample heating is presumably one of the most effective methods for stopping enzymatic activities. However, a homogenate containing Laemmli buffer cannot be applied to isoelectric focusing or tryptic digestion, which both is possible with DIVE homogenates.

Comparing the number of identified proteins in pancreas tissue it was observed that DTH resulted in a higher number of identified proteins compared to MTH (Fig. 5 A, DTH: 1743 proteins (+/− 173), MTH: 1467 proteins (+/− 138)). With DTH a considerably higher number of proteins (1418 proteins, Fig. 5 B) were identified in all three replicates compared to MTH (1116 proteins, Fig. 5 B). In addition, a comparison of the proteins identified in all biological samples showed that 1092 proteins (75%) were identified in both DTH and MTH. In total 24 proteins (2%) were only identified after MTH, whereas a 326 proteins (23%) were exclusively identified after DTH (Fig. 5 C). This is comparable with the results from the LC–MS/MS analysis of the tonsil homogenates and confirmed that a considerably higher number of proteins are accessible with DTH compared to MTH.

For comparing degradation and the recovery rate, alpha-casein proteins were spiked in equal amounts to the wash-bottle of the DH and to the lysis buffer in case of conventional homogenization using a bead mill (MH, Fig. S28). Equal amounts of both DH and MH were subjected to SDS-PAGE, followed by tryptic in-gel digestion and quantitative LC–MS/MS analysis. Results of LC–MS/MS analysis revealed that on average a significantly higher yield of intact alpha-S1-casein species were obtained in case of DTH (Fig. 6 A). In addition, a significantly higher yield of alpha-S1-casein species with a molecular weight less than 14 kDa were detected in MH (Fig. 6 B). A comparison of the number of identified casein phosphopeptides in DH and MH revealed that a significantly higher number of phosphopeptides were identified in DH (Fig. 6 C). Since casein proteins were spiked to the wash-bottle and the lysis buffer prior to DTH and MTH, both the significantly higher yield of intact casein species and the significantly higher number of identified casein phosphopeptides in DH are most probably due to a much shorter exposure time to enzymatic degradation reactions and less sample loss during DTH, because no particles were present, which had to be removed by centrifugation in contrast to MTH.

4. Conclusion

The results of the 2DE and the SDS-PAGE analysis showed that with DIVE tissue homogenization (DTH) a significantly higher number of intact protein species are yielded compared to conventional mechanical tissue

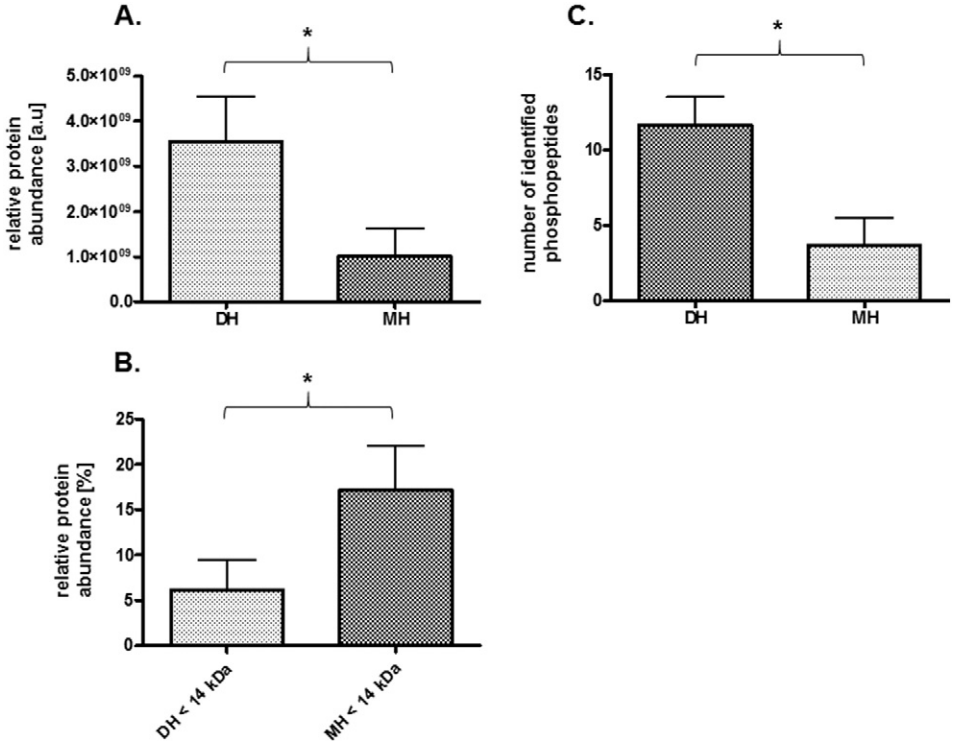

Fig. 6. Statistical analysis of the LC–MS/MS data from the SDS-PAGE of the DIVE homogenate (DH) and the mechanical homogenate (MH) from rat pancreas (n = 3) spiked with alpha-casein. A: Histogram (mean with standard deviation (SD)) showing the average relative protein abundance of intact alpha-S1-casein protein species detected in the appropriate SDS-PAGE bands of DH and MH, *: p = 0.02 (t-test). B: Histogram (mean with SD) showing the percentage of alpha-S1-casein species with a molecular weight less than 14 kDa detected in appropriate SDS-PAGE bands of DH and MH, *: p = 0.031 (t-test). C: Histogram (mean with SD) showing the number of identified alpha-S2-casein phosphopeptides after DIVE homogenization (DTH) and mechanical homogenization (MTH), *: p = 0.038 (t-test).

homogenization (MTH). The ultrafast transfer of proteins from the tissue into a frozen aerosol condensate within milliseconds decreases the overall time intact protein species are exposed to enzymatic degradation reactions during DTH. The results from the spiking experiments confirmed the findings and in addition indicated a larger recovery rate of phosphopeptides in DH compared to MH. A huge advantage of DTH in comparison to MTH is the high quality of the homogenate, which is characterized by the absence of particles like cell debris. The presence of particles in the homogenate of MTH requires an additional centrifugation step and shows that not all parts of the tissue were successfully homogenized. Consequently, the results of both tonsil and pancreas tissue homogenization by DIVE (DTH) showed that not only the total number of identified protein species was much larger, but also a considerably larger number of protein species were reproducibly identified in all biological replicates compared to conventional tissue homogenization (MTH). Lower yield for the MH may be the result of proteins discarded in the centrifugation pellet due to their adsorption to insoluble particles. We therefore hypothesize that DTH allows a more representative view of the original *in-vivo* composition of protein species in tissue proteomes.

The mass spectrometry proteomics data have been deposited to the ProteomeXchange Consortium via the PRIDE partner repository with the dataset identifier PXD003434

Supplementary data to this article can be found online at http://dx.doi.org/10.1016/j.jprot.2015.12.029.

Conflict of interest

All authors declare no financial/commercial conflicts of interest.

Acknowledgment

We thank the SUREPIRL project (ERC advanced grant, project reference: 291630) for financial support.

References

[1] T.M. Karve, A.K. Cheema, Small changes huge impact: the role of protein posttranslational modifications in cellular homeostasis and disease, J. Amino Acids 2011 (2011) 207691.
[2] R. Bischoff, H. Schluter, Amino acids: chemistry, functionality and selected non-enzymatic post-translational modifications, J. Proteome 75 (2012) 2275–2296.
[3] Y.C. Wang, S.E. Peterson, J.F. Loring, Protein post-translational modifications and regulation of pluripotency in human stem cells, Cell Res. 24 (2014) 143–160.
[4] I. Dalle-Donne, G. Aldini, M. Carini, R. Colombo, R. Rossi, A. Milzani, Protein carbonylation, cellular dysfunction, and disease progression, J. Cell. Mol. Med. 10 (2006) 389–406.
[5] T.A. Freeman, J. Parvizi, C.J. Della Valle, M.J. Steinbeck, Reactive oxygen and nitrogen species induce protein and DNA modifications driving arthrofibrosis following total knee arthroplasty, Fibrogenesis Tissue Repair 2 (2009) 5.
[6] G.O. Osoata, S. Yamamura, M. Ito, C. Vuppusetty, I.M. Adcock, P.J. Barnes, et al., Nitration of distinct tyrosine residues causes inactivation of histone deacetylase 2, Biochem. Biophys. Res. Commun. 384 (2009) 366–371.
[7] A.G. Madian, F.E. Regnier, Proteomic identification of carbonylated proteins and their oxidation sites, J. Proteome Res. 9 (2010) 3766–3780.
[8] P. Jungblut, B. Thiede, U. Zimny-Arndt, E.C. Muller, C. Scheler, B. Wittmann-Liebold, et al., Resolution power of two-dimensional electrophoresis and identification of proteins from gels, Electrophoresis 17 (1996) 839–847.
[9] H. Schluter, R. Apweiler, H.G. Holzhutter, P.R. Jungblut, Finding one's way in proteomics: a protein species nomenclature, Chem. Cent. J. 3 (2009) 11.
[10] P.R. Jungblut, Back to the future—the value of single protein species investigations, Proteomics 13 (2013) 3103–3105.
[11] A. Bodzon-Kulakowska, A. Bierczynska-Krzysik, T. Dylag, A. Drabik, P. Suder, M. Noga, et al., Methods for samples preparation in proteomic research, J. Chromatogr. B Anal. Technol. Biomed. Life Sci. 849 (2007) 1–31.
[12] B. Canas, C. Pineiro, E. Calvo, D. Lopez-Ferrer, J.M. Gallardo, Trends in sample preparation for classical and second generation proteomics, J. Chromatogr. A 1153 (2007) 235–258.
[13] C.B. Rountree, C.A. Van Kirk, H. You, W. Ding, H. Dang, H.D. VanGuilder, et al., Clinical application for the preservation of phospho-proteins through in-situ tissue stabilization, Proteome Sci. 8 (2010) 61.
[14] M.L. Colgrave, L. Xi, S.A. Lehnert, T. Flatscher-Bader, H. Wadensten, A. Nilsson, et al., Neuropeptide profiling of the bovine hypothalamus: thermal stabilization is an effective tool in inhibiting post-mortem degradation, Proteomics 11 (2011) 1264–1276.
[15] C. Stingl, M. Soderquist, O. Karlsson, M. Boren, T.M. Luider, Uncovering effects of ex vivo protease activity during proteomics and peptidomics sample extraction in rat brain tissue by oxygen-18 labeling, J. Proteome Res. 13 (2014) 2807–2817.
[16] S. RK, Protein Purification: Principles and Practice, third ed. Springer-Verlag, New York, 1994 (1994).
[17] M. Svensson, M. Boren, K. Skold, M. Falth, B. Sjogren, M. Andersson, et al., Heat stabilization of the tissue proteome: a new technology for improved proteomics, J. Proteome Res. 8 (2009) 974–981.
[18] J. Yi, C. Kim, C.A. Gelfand, Inhibition of intrinsic proteolytic activities moderates preanalytical variability and instability of human plasma, J. Proteome Res. 6 (2007) 1768–1781.
[19] V. Espina, C. Mueller, K. Edmiston, M. Sciro, E.F. Petricoin, L.A. Liotta, Tissue is alive: new technologies are needed to address the problems of protein biomarker preanalytical variability, Proteomics Clin. Appl. 3 (2009) 874–882.
[20] S. Amini-Nik, D. Kraemer, M.L. Cowan, K. Gunaratne, P. Nadesan, B.A. Alman, et al., Ultrafast mid-IR laser scalpel: protein signals of the fundamental limits to minimally invasive surgery, PLoS ONE 5 (2010).
[21] M. Kwiatkowski, M. Wurlitzer, M. Omidi, L. Ren, S. Kruber, R. Nimer, et al., Ultrafast extraction of proteins from tissues using desorption by impulsive vibrational excitation, Angew. Chem. 54 (2015) 285–288.
[22] K. Franjic, M.L. Cowan, D. Kraemer, R.J. Miller, Laser selective cutting of biological tissues by impulsive heat deposition through ultrafast vibrational excitations, Opt. Express 17 (2009) 22937–22959.
[23] K. Franjic, D. Miller, Vibrationally excited ultrafast thermodynamic phase transitions at the water/air interface, Phys. Chem. Chem. Phys. 12 (2010) 5225–5239.
[24] A. Bottcher, S. Kucher, R. Knecht, N. Jowett, P. Krotz, R. Reimer, et al., Reduction of thermocoagulative injury via use of a picosecond infrared laser (PIRL) in laryngeal tissues, Eur. Arch. Otorhinolaryngol. 272 (2015) 941–948.
[25] L. Ren, W.D. Robertson, R. Reimer, C. Heinze, C. Schneider, D. Eggert, et al., Towards instantaneous cellular level bio diagnosis: laser extraction and imaging of biological entities with conserved integrity and activity, Nanotechnology 26 (2015) 284001.
[26] M. Mulisch, U. Welsch, Romeis Mikroskopische Technik, 18 ed. Spektrum Akademischer Verlag, Heidelberg, 2010.
[27] J. Klose, U. Kobalz, Two-dimensional electrophoresis of proteins: an updated protocol and implications for a functional analysis of the genome, Electrophoresis 16 (1995) 1034–1059.
[28] M. Berth, F.M. Moser, M. Kolbe, J. Bernhardt, The state of the art in the analysis of two-dimensional gel electrophoresis images, Appl. Microbiol. Biotechnol. 76 (2007) 1223–1243.
[29] A. Shevchenko, H. Tomas, J. Havlis, J.V. Olsen, M. Mann, In-gel digestion for mass spectrometric characterization of proteins and proteomes, Nat. Protoc. 1 (2006) 2856–2860.
[30] J. Cox, M. Mann, MaxQuant enables high peptide identification rates, individualized p.p.b.-range mass accuracies and proteome-wide protein quantification, Nat. Biotechnol. 26 (2008) 1367–1372.
[31] J. Cox, M.Y. Hein, C.A. Luber, I. Paron, N. Nagaraj, M. Mann, Accurate proteome-wide label-free quantification by delayed normalization and maximal peptide ratio extraction, termed MaxLFQ, Mol. Cell. Proteomics 13 (2014) 2513–2526.
[32] W. Huang da, B.T. Sherman, R.A. Lempicki, Bioinformatics enrichment tools: paths toward the comprehensive functional analysis of large gene lists, Nucleic Acids Res. 37 (2009) 1–13.
[33] W. Huang da, B.T. Sherman, R.A. Lempicki, Systematic and integrative analysis of large gene lists using DAVID bioinformatics resources, Nat. Protoc. 4 (2009) 44–57.
[34] J. Seo, J. Jeong, Y.M. Kim, N. Hwang, E. Paek, K.J. Lee, Strategy for comprehensive identification of post-translational modifications in cellular proteins, including low abundant modifications: application to glyceraldehyde-3-phosphate dehydrogenase, J. Proteome Res. 7 (2008) 587–602.
[35] C. Choudhary, C. Kumar, F. Gnad, M.L. Nielsen, M. Rehman, T.C. Walther, et al., Lysine acetylation targets protein complexes and co-regulates major cellular functions, Science 325 (2009) 834–840.
[36] Y. Bian, C. Song, K. Cheng, M. Dong, F. Wang, J. Huang, et al., An enzyme assisted RP-RPLC approach for in-depth analysis of human liver phosphoproteome, J. Proteome 96 (2014) 253–262.
[37] P. Feist, A.B. Hummon, Proteomic challenges: sample preparation techniques for microgram-quantity protein analysis from biological samples, Int. J. Mol. Sci. 16 (2015) 3537–3563.
[38] G.J. Laurent, Dynamic state of collagen: pathways of collagen degradation in vivo and their possible role in regulation of collagen mass, Am. J. Physiol. 252 (1987) C1–C9.